

Article

A Hybrid Framework Model Based on Wavelet Neural Network with Improved Fruit Fly Optimization Algorithm for Traffic Flow Prediction

Qingyong Zhang ¹, Changwu Li ¹ , Conghui Yin ¹, Hang Zhang ^{2,*} and Fuwen Su ³

¹ School of Automation, Wuhan University of Technology, Wuhan 430070, China; qyzhang@whut.edu.cn (Q.Z.); 265639@whut.edu.cn (C.L.); conghuiyin@whut.edu.cn (C.Y.)

² School of Transportation and Logistics Engineering, Wuhan University of Technology, Wuhan 430063, China

³ School of Information Engineering, Wuhan University of Technology, Wuhan 430070, China; fwsu@whut.edu.cn

* Correspondence: zh2022@whut.edu.cn

Abstract: Accurate traffic flow prediction can provide sufficient information for the formation of symmetric traffic flow. To overcome the problem that the basic fruit fly optimization algorithm (FOA) is easy to fall into local optimum and the search method is single, an improved fruit fly optimization algorithm (IFOA) based on parallel search strategy and group cooperation strategy is proposed. The multi-swarm mechanism is introduced in the parallel search strategy, in which each subswarm is independent and multiple center positions are determined in the iterative process, thereby avoiding the problems of reduced diversity and premature convergence. To increase communication between fruit fly subswarms, the informative fruit flies selected from subswarms are guided by the randomly generated binary fruit fly to achieve the crossover operation in the group cooperation strategy. Then a hybrid framework model based on wavelet neural network (WNN) with IFOA (IFOA-WNN) for traffic flow prediction is designed, in which IFOA is applied to explore appropriate structure parameters for WNN to achieve better prediction performance. The simulation results verify that the IFOA can provide high-quality structural parameters for WNN, and the hybrid IFOA-WNN prediction model can achieve higher prediction accuracy and stability than the compared methods.

Keywords: traffic flow prediction; wavelet neural network; fruit fly optimization algorithm; group cooperation strategy; parallel search strategy



Citation: Zhang, Q.; Li, C.; Yin, C.; Zhang, H.; Su, F. A Hybrid Framework Model Based on Wavelet Neural Network with Improved Fruit Fly Optimization Algorithm for Traffic Flow Prediction. *Symmetry* **2022**, *14*, 1333. <https://doi.org/10.3390/sym14071333>

Academic Editor: Marco Montemurro

Received: 28 May 2022

Accepted: 23 June 2022

Published: 28 June 2022

Publisher's Note: MDPI stays neutral with regard to jurisdictional claims in published maps and institutional affiliations.



Copyright: © 2022 by the authors. Licensee MDPI, Basel, Switzerland. This article is an open access article distributed under the terms and conditions of the Creative Commons Attribution (CC BY) license (<https://creativecommons.org/licenses/by/4.0/>).

1. Introduction

Accurate traffic flow prediction has become an important research focus of intelligent transportation systems [1]. It can help traffic managers make reasonable traffic decisions and provide more information to travelers to help them adjust their routes and change travel plans in time. Moreover, the traffic flow prediction is also of great benefit for maintaining the traffic flow in a symmetry condition. The formation of symmetrical traffic flow can speed up the efficiency of traffic flow and relieve traffic congestion on arterials. However, affected by meteorological conditions, traffic accidents, and road maintenance construction, traffic flow presents a high degree of dynamics, randomness, and chaos [2], making traffic flow prediction a challenging problem.

Many researchers and scholars have studied many methods to enhance prediction performance in the past decade. The main traffic flow prediction methods can be roughly classified into three categories: traditional statistical learning methods, artificial neural networks (NNs) methods, and hybrid NNs methods. Traditional statistical learning methods, such as Kalman filtering [3], autoregressive integrated moving average [4] and Bayesian method [5], are suitable for processing simple and low-dimensional traffic flow. The main reason is that these methods are limited by the assumption of stationary processes and linear combinations of previous observations, making them difficult to predict the dynamics

of time series [6]. Therefore, the traditional statistical learning models are less effective in predicting traffic flow sequences with uncertainty and complexity and cannot meet the current practical engineering needs. In this context, the NNs [7,8] are widely used in traffic flow prediction tasks due to their uncertainty and nonlinear extraction ability. Alqatawna et al. [9] introduced the NN as a predictive tool to explore the leading cause of traffic accidents from multiple data sources. Sharma et al. [10] proposed the back propagation neural network (BPNN) for traffic flow prediction of two-lane undivided roads, and the experiments demonstrated that the prediction performance of the BPNN is better than the machine learning methods. Although the NNs methods improve the prediction accuracy, their generalization ability and prediction effectiveness are greatly influenced by the network hyperparameters [11], and the appropriate network structure parameters require several experiments to determine.

Swarm intelligence is an intelligent behavior formed by the interaction between simple individuals and between individuals and the environment. The swarm intelligence optimization algorithm can provide some new solutions to traffic prediction problems. Swarm intelligence optimization algorithms, such as particle swarm optimization algorithm [12], genetic algorithm (GA) [13], ant colony optimization algorithm [14], artificial bee colony optimization algorithm [15], FOA [16], grey wolf optimizer algorithm [17], whale optimization algorithm [18], have fewer parameters and simple evolutionary iteration process. Their operation speed is fast, and their global search ability is strong, enabling them to be suitable for solving high-dimensional and multi-objective optimization problems. In order to improve the shortcomings of NNs and improve the generalization ability, many studies have introduced a hybrid framework based on NNs and swarm intelligence algorithms for traffic flow prediction [19–21]. The core of the hybrid NN model is to use the swarm intelligence algorithm to adaptively optimize the layer connections and layer nodes in the neural network. The traffic flow prediction accuracy can be improved in a complementary way through the organic combination of swarm intelligence algorithms and the NNs. Abolghase et al. [22] investigated a modified Elman recurrent neural network model that uses GA for process optimization, thus allowing the model to prevent getting stuck in local minima and find solutions quickly. Yan et al. [23] introduced a hybrid NNs framework for traffic flow prediction where an adaptive FOA is used to optimize the model's parameters. Li et al. [24] used the firefly algorithm to obtain better initial network weights and thresholds, thereby making up for the random defects of the BPNN. Peng et al. [25] proposed a traffic prediction model based on GA. The original traffic flow data is first preprocessed by wavelet denoising method. Then, the BP neural network is optimized by GA, and the optimized prediction model has better accuracy. In summary, combining swarm intelligence algorithms with the NNs methods is an effective measure to improve traffic flow prediction performance and is receiving increasing attention from research scholars.

The number of vehicles in the road segments scene has a large order of magnitude and strong temporal correlation. WNN [26] is a neural network based on the topology of the BPNN, with a three-layer network structure, and the activation function of the hidden layer is replaced by a wavelet function. Because the WNN integrates the advantages of the fast convergence speed of the NNs and the time frequency local analysis of the wavelet analysis [27], the WNN can more accurately approximate the time series of traffic flow in the road segments. However, the random selection of its hyperparameters makes the WNN easy to fall into the local optimum in the gradient descent process [28]. The FOA can be used to solve the drawbacks of WNN. The FOA simulates the process of fruit fly foraging through two iterative processes of smell search and visual search, and continuously optimizes parameters to obtain the optimal solution [29,30]. The structure of the FOA algorithm is relatively simple, requires few parameters, and has the advantages of strong search ability, small computational complexity, and fast convergence performance [31]. Therefore, this study proposes a hybrid prediction framework based on the IFOA and the WNN to realize traffic flow prediction tasks in the road segments scene. The main contributions of this paper are as follows,

- (1) To solve the problem that the FOA easily falls into local optimum, the IFOA using parallel search strategy and group cooperation strategy is designed to improve the quality solution.
- (2) A hybrid prediction model based on WNN with IFOA (IFOA-WNN) is introduced, which combines the advantages of the nonlinear fitting ability and the fast convergence ability to predict the traffic flow prediction in the road segments scene.
- (3) Experiments are carried out on the real road dataset. The experiment results show that the IFOA can select appropriate structure parameters for WNN, and the proposed IFOA-WNN model can make accurate prediction results.

The rest of the paper is organized as follows. Section 2 presents some basic knowledge. In Section 3, the parallel search strategy and group cooperation strategy are developed in IFOA. Section 4 describes the details of our proposed IFOA-WNN model. The experiment results are presented in Section 5, and Section 6 concludes this paper.

2. Basic Knowledge

2.1. Mathematical Model of Traffic Flow in Road Segments

The traffic flow characteristics of road segments include vehicle flow, average speed, and vehicle density. For different road segments, the traffic flow change and the critical value of the traffic flow index [32] are different. A single-lane road segment is with only one entry lane and one exit lane. As shown in Figure 1, the traffic flow of the road segment is determined by the number of vehicles entering and leaving the road segment within $5(n - 1) \sim 5n$ minutes, and the number of vehicles included in the road segment at the previous moments. Therefore, the number of vehicles on the road segment at the moment k can be calculated as follows.

$$Q(k) = \sum_{i=1}^k q_{in}(i) - \sum_{i=1}^k q_{out}(i) + q_0 \tag{1}$$

where q_0 is the number of vehicles included in the initial time; and $q_{in}(i)$ and $q_{out}(i)$ are the number of vehicles entering and leaving the road segment, respectively.

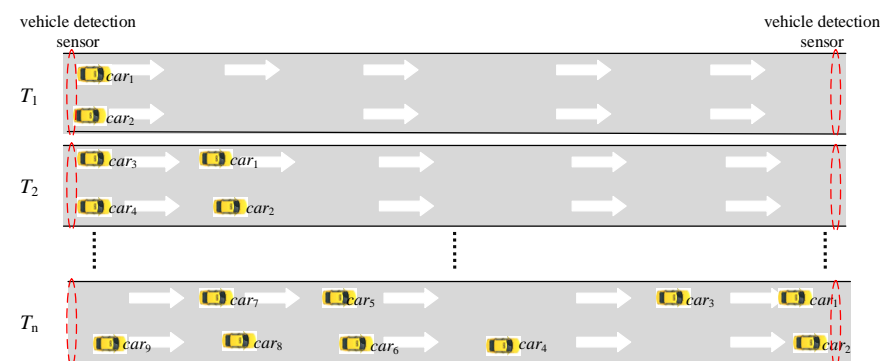


Figure 1. Extraction of the number of vehicles on a single-lane road segment.

The extraction of the number of vehicles on a multi-channel road segment is shown in Figure 2. In order to predict the number of vehicles in this multi-channel road segment, it is necessary to set up multiple detection sensors on the main line, on-ramp, off-ramp, and intersection, and use the data collected from these sensors to calculate the number of vehicles on the complex road segments. The number of vehicles at the moment k is defined as follows.

$$\bar{Q}(k) = \sum_{i=1}^N \sum_{s=0}^k \bar{q}_{in}(i, s) - \sum_{j=1}^M \sum_{s=0}^k \bar{q}_{out}(j, s) + \bar{q}_0 \tag{2}$$

where $\bar{Q}(k)$ is the total vehicle volume on the complex road segment; \bar{q}_0 is the number of vehicles at the initial moment; and $\bar{q}_{in}(i, s)$ and $\bar{q}_{out}(j, s)$ are the number of vehicles entering and exiting the section at the s^{th} moment from the i^{th} on-ramp and j^{th} off-ramp, respectively.

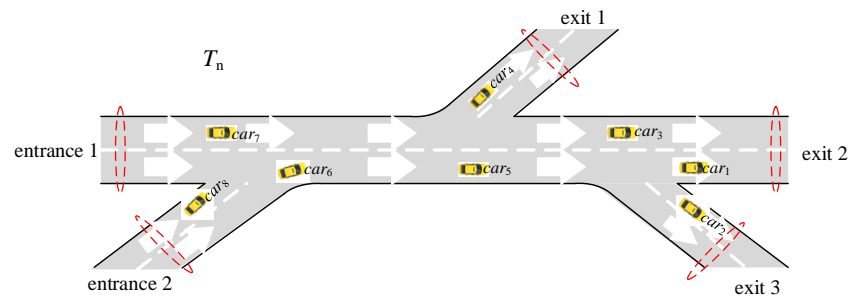


Figure 2. Extraction of the number of vehicles on a multi-channel road segment.

2.2. Fruit Fly Optimization Algorithm

The Fruit Fly Optimization Algorithm (FOA) is a swarm intelligence optimization algorithm based on the foraging behavior of the fruit flies. When searching for food, a group of the fruit flies first relies on the sense of smell to determine the approximate distance between the fruit fly itself and the target food. The overall idea of the FOA algorithm in solving the problem of finding the optimal solution is similar to that of a fruit fly population searching for food.

The location information of the best fruit fly in the fruit fly population is determined by the smell search method. However, the visual search method is different in that all the fruit flies in the population search randomly outward from the location information of the optimal fruit fly, and then the two steps of smell search and visual search are cycled until the optimal solution of the problem is obtained. To describe the FOA algorithm in the more detail, we take the optimization problem of a binary function $g(x, y)$ as an example. The process of solving the optimal solution of a binary function by FOA can be divided into the following steps.

- Step 1. Initializing the parameters of the fruit fly swarm. Initialize the number N of fruit flies in the swarm, the initial position (x_0, y_0) of the fruit fly swarm, the search step size L , and the maximum number T_{max} of iterations.
- Step 2. Smell search process. The fruit fly swarm starts from the initial position (x_0, y_0) and searches randomly in all directions with step L to get the updated position (x_i, y_i) , $i = 1, 2, \dots, N$.

$$x_i = x_0 + L \times Rand() \tag{3}$$

$$y_i = y_0 + L \times Rand() \tag{4}$$

where $Rand()$ is a random value of $(0, 1)$. After completing the random search, the smell concentration judgment value $Smell_i = g(x_i, y_i)$ of the current position of the fruit fly is calculated, and the function $g(\cdot)$ is the smell concentration function.

- Step 3. Visual search process. The fruit fly with the best smell concentration judgment value $bestSmell$ in the swarm is selected as the optimal fruit fly, and the global optimal A value and the global optimal fruit fly location information are updated when the optimal fruit fly's $bestSmell$ is better than the global optimal value $Smellbest$. The update process is given by the following equation.

$$[bestSmell, bestIndex] = \max(Smell_1, Smell_2, \dots, Smell_N) \tag{5}$$

$$Smellbest = bestSmell \tag{6}$$

$$x_0 = bestIndex_x \tag{7}$$

$$y_0 = bestIndex_y \tag{8}$$

Step 4. Determine the termination condition. If the maximum number of iterations is reached, the algorithm terminates and outputs the optimal solution ($bestIndex_x, bestIndex_y$) that leads to the optimal value of the function $g(x, y)$; otherwise, it returns to step 2.

3. Improved Fruit Fly Optimization Algorithm

3.1. Parallel Search and Group Cooperation Strategies in IFOA

Although the FOA has strong search ability, it is easy to fall into local optimum. Mainly because of the following two problems, (1) During the entire iterative optimization process, the fruit fly swarm moves to the position of the current optimal fruit fly individual. Once the optimal position of this iteration is determined, all the fruit fly individuals will gather, which will weaken the diversity of the swarm. (2) A single search operation often makes the new solutions generated in the iterative process more similar. The fruit fly individual in the swarm tends to be consistent, making the search process easy to fall into a local optimum.

In order to solve the above problems, IFOA which uses parallel search strategy and group cooperation strategy is developed to improve the solution quality of the algorithm.

(1) Parallel search strategy

By introducing a multi-swarm mechanism and determining multiple center locations in the iterative process, the fruit fly swarm can be effectively avoided from concentrating near one central location, thus maintaining the diversity of the swarm and improving the global search ability of the algorithm. The parallel search strategy performs search food in multiple fruit fly subswarms and then compares the optimal solutions of each subswarm to determine the global optimal solution.

(2) Group cooperation strategy

If each subswarm searches independently, there will be no communication between subswarms, resulting in lower search efficiency. Therefore, the group cooperation strategy is designed to solve this problem. The main steps are as follows.

- Step 1. The subswarms are sorted in descending order according to the fitness function value and select the subswarm as the invariant subswarms whose fitness function value is in the top 50% for group cooperation strategy.
- Step 2. If the number of the subswarms is M , the p^{th} subswarm and the $(M - p + 1)^{th}$ subswarm after sorting will be cross-transformed, $p = 1, 2, \dots, M/2$.
- Step 3. The fruit fly with optimal value in a subswarm is chosen as the information fruit fly of the subswarm. A binary crossover fruit fly and the information fruit fly of the subswarm have the same length. The crossover fruit fly is randomly generated to perform the crossover operation on the p^{th} subswarm and the $(M - p + 1)^{th}$ subswarm informative fruit flies. The informative fruit fly of the p^{th} subswarm does not change, and the informative fruit fly of the $(M - p + 1)^{th}$ subswarm changes as the crossover operation.

As shown in Figure 3, we take a five-dimensional fruit fly individual as an example. For the position where the information carried by the binary crossover fruit fly is 1, the parameter values of the corresponding positions of the two information fruit flies are exchanged. The position of the information carried by the binary crossover fruit fly is 0, and no crossover operation is performed. $x_{A1}, x_{A2}, \dots, x_{A5}$ is the position information of the p^{th} information fruit fly. $x_{B1}, x_{B2}, \dots, x_{B5}$ is the position information of the $(M - p + 1)^{th}$ information fruit fly.

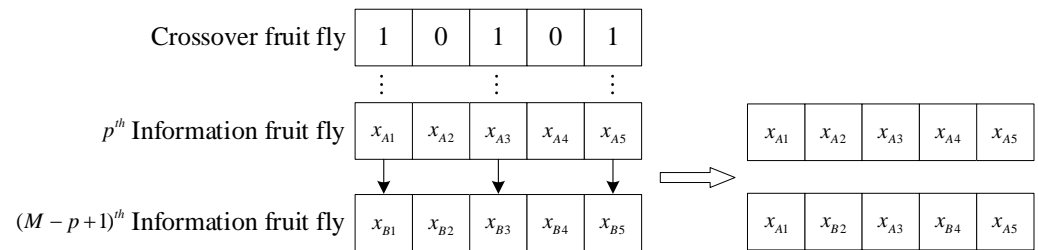


Figure 3. The information fruit fly crossover diagram.

3.2. Execution Steps of the IFOA

Similarly, taking the optimization problem of a binary function $g(x, y)$ as an example, the process of solving the optimal solution when the function reaches the optimal value by IFOA can be expressed as the following steps. The flowchart of the IFOA is shown in Figure 4.

- Step 1. Initializing parameters of the fruit fly swarm. The number of subswarms is initialized as M , and the number of fruit fly in each subswarm is set to N . The fruit fly swarm can be expressed as $F = \{F_1, F_2, \dots, F_M\}$. Therefore, each fruit fly subswarm can be expressed as $F_i = \{(x_{i,1}, y_{i,1}), (x_{i,2}, y_{i,2}), \dots, (x_{i,N}, y_{i,N})\}$, $i = 1, 2, \dots, M$. The initial position of the swarm is set to (x_0, y_0) , the initial position of each subswarm is initialized as (x_i, y_i) , $i = 1, 2, \dots, M$. The search step size is L and the maximum iterations is set to T_{\max} .
- Step 2. Smell search process. Distance to each fruit fly is randomly assigned to carry out the search process. The initial position of each fruit fly is $(x_{i,j}, y_{i,j})$, $i = 1, 2, \dots, M$, and $j = 1, 2, \dots, N$, and each subswarm performs this process independently.

$$x_{i,j} = x_i + L \times \text{Rand}() \quad (9)$$

$$y_{i,j} = y_i + L \times \text{Rand}() \quad (10)$$

where $\text{Rand}()$ is a random value of $(0, 1)$. After completing the random search, the smell concentration judgment value $\text{Smell}_{i,j} = g(x_{i,j}, y_{i,j})$ of the current position of the fruit fly is calculated. In this paper, the smell concentration judgment value $\text{Smell}_{i,j}$ of different fruit flies is the prediction error value calculated by applying the WNN network hyperparameters carried by different fruit flies to the WNN for traffic flow prediction. In this case, the smaller the value of $\text{Smell}_{i,j}$, the better.

- Step 3. Visual search process with the group cooperation strategy. Firstly, we find the optimal value bestSmell_i and optimal solution $\text{bestIndex}_i = (\text{bestIndex}_{i,x}, \text{bestIndex}_{i,y})$ in each subpopulation, and the information exchange operation is executed between subswarms according to the group cooperation strategy. Finally, we find the global optimal value smellbest and optimal solution bestIndex in the whole swarm.

$$[\text{bestSmell}_i, \text{bestIndex}_i] = \min(\text{Smell}_{i,1}, \text{Smell}_{i,2}, \dots, \text{Smell}_{i,N}) \quad (11)$$

$$\text{Smellbest} = \min(\text{bestSmell}_1, \text{bestSmell}_2, \dots, \text{bestSmell}_M) \quad (12)$$

$$\text{bestIndex} = \text{bestIndex}(\text{Smellbest}) \quad (13)$$

$$x_i = \text{bestIndex}_{i,x} \quad (14)$$

$$y_i = \text{bestIndex}_{i,y} \quad (15)$$

- Step 4. Determining the termination condition. If the maximum number of iterations T_{\max} is not reached, the position of each subswarm is updated. Then enter the iteration, repeat step 2 to 4 until the number of iterations reaches T_{\max} . Otherwise, the algorithm

terminates and outputs the optimal solution (x_0, y_0) that leads to the optimal value of the function $g(x, y)$.

$$x_0 = bestIndex_x \tag{16}$$

$$y_0 = bestIndex_y \tag{17}$$

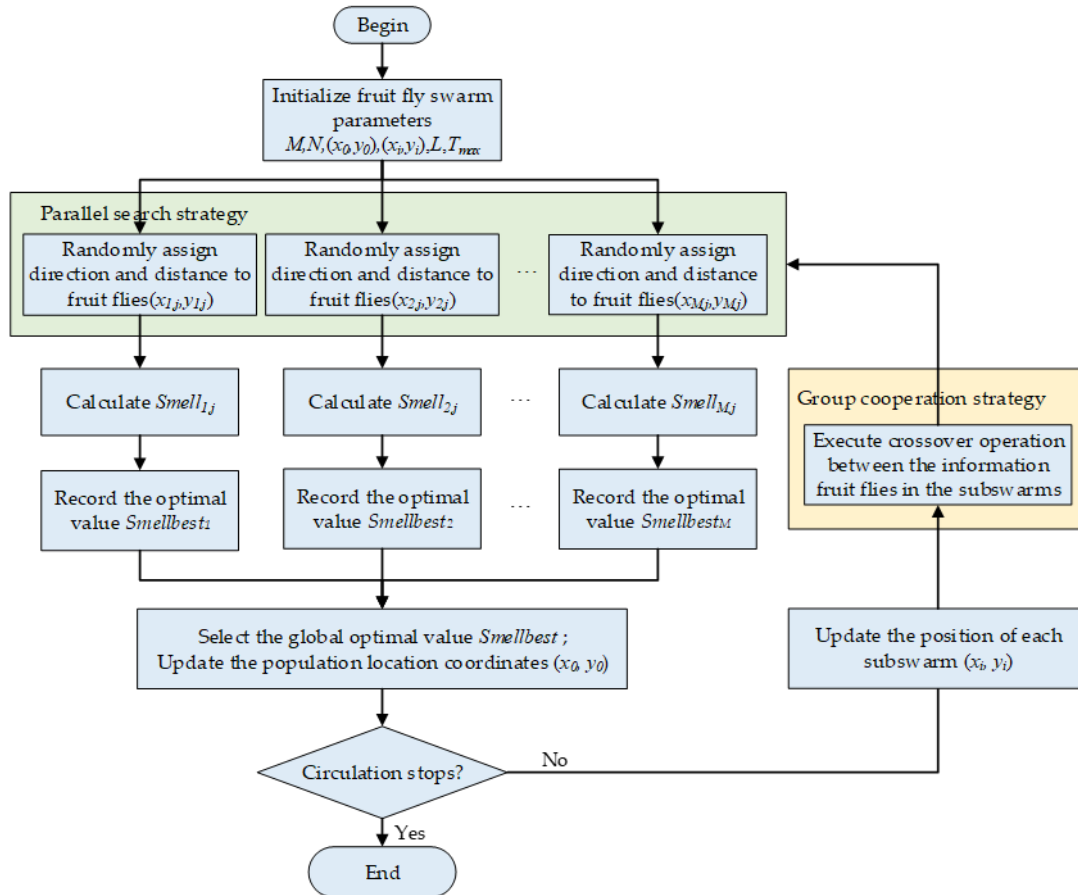


Figure 4. The flowchart of the IFOA.

4. The Hybrid IFOA-WNN Model for Traffic Prediction

4.1. Wavelet Neural Network

WNN adds wavelet transform technology based on NNs. Compared with BPNN, it can simplify the training process, and has more significant advantages and excellent learning ability for predicting time series. Therefore, WNN is chosen to learn the nonlinear and temporal characteristics of road segment traffic flow in our study. The prediction process of WNN is divided into two parts: forward calculation of input signal and error back propagation learning.

- (1) Forward calculation of input signal

The hidden layer output $hid(j)$ is defined as follows.

$$hid(j) = h \left(\frac{\sum_{i=1}^{N_{input}} w_{ij}y(t-i) - B_j}{A_j} \right), j = 1, 2, \dots, N_{hid} \tag{18}$$

where $u(t) = [y(t-1), y(t-2), \dots, y(t-N_{input})]^T$ is the input data; N_{hid} is the number of hidden units; $h(\cdot)$ is the wavelet basis function; w_{ij} is the weight matrix between the

input layer and the hidden layer; A_j and B_j are the scaling factor and translation factor of the wavelet basis function, respectively.

The output $\hat{y}(t)$ of the WNN is calculated as follows.

$$\hat{y}(t) = \sum_{j=1}^m w_{jk} \text{hid}(j), k = 1, 2, \dots, N_{out} \quad (19)$$

where w_{jk} is the weight matrix between the hidden layer and the output layer; N_{out} is the number of output units.

The error between the output and the true value and the loss function is denoted as follows.

$$e(t) = \hat{y}(t) - y(t) \quad (20)$$

$$E = \frac{1}{2} e(t)^2 \quad (21)$$

(2) Error back propagation learning

The calculation formulas of the weights and wavelet factors of the WNN are follows.

$$\begin{aligned} w_{ij}^{(d+1)} &= w_{ij}^{(d)} + \Delta w_{ij}^{(d+1)} \\ w_{jk}^{(d+1)} &= w_{jk}^{(d)} + \Delta w_{jk}^{(d+1)} \\ A_j^{(d+1)} &= A_j^{(d)} + \Delta A_j^{(d+1)} \\ B_j^{(d+1)} &= B_j^{(d)} + \Delta B_j^{(d+1)} \end{aligned} \quad (22)$$

where d is the iterative times; Δw_{ij} , Δw_{jk} , ΔA_j , ΔB_j represent the adjustment amount in the $d + 1^{th}$ iteration process, and its mathematical formula is as follows.

$$\begin{aligned} \Delta w_{ij}^{(d+1)} &= -\eta \partial E / \partial w_{ij}^{(d)} \\ \Delta w_{jk}^{(d+1)} &= -\eta \partial E / \partial w_{jk}^{(d)} \\ \Delta A_j^{(d+1)} &= -\eta \partial E / \partial A_j^{(d)} \\ \Delta B_j^{(d+1)} &= -\eta \partial E / \partial B_j^{(d)} \end{aligned} \quad (23)$$

where η is the learning rate.

In the process of back propagation, the weight parameters w_{ij} , w_{jk} , scaling factor A_j and translation factor B_j in the WNN are continuously updated under the guidance of the loss function, making the model's predicted value constantly close to the real value. However, the WNN is sensitive to the initial value of the structural parameters, so our proposed IFOA needs to be used to adjust the initial parameters of the WNN to achieve a better prediction effect.

4.2. The Hybrid IFOA-WNN Model

Based on the strong global search ability of IFOA and the nonlinear capture ability of WNN, a hybrid structure IFOA-WNN model is established for traffic flow prediction in the road segment scene. The IFOA-WNN prediction model is divided into two parts, including the IFOA, to optimize the structural parameters of the WNN, and the optimized WNN used to predict the traffic flow.

In the prediction process, the input of the WNN is the number of vehicles passing through a section segment at multiple historical sampling times, and the output value of the WNN is the predicted value at the next moment. It can be expressed to predict the traffic flow of the next moment \hat{y}_t through the traffic flow of the historical moment

$\mathbf{u}(t) = [y_{t-N_{input}+1}, \dots, y_{t-1}, y_t]^T$. The main structural parameters of the WNN include the input layer units N_{input} , the hidden layer units N_{hid} , the learning rate of connection weights LR_w , the learning rate of translation factors LR_A , and the learning rate of scaling factors LR_B . These structural parameters are used as the position vector of the IFOA, and the position vector \mathbf{P} of the individual fruit fly and the fitness function can be denoted as follows.

$$\mathbf{P} = [N_{input}, N_{hid}, LR_w, LR_A, LR_B] \quad (24)$$

$$MAE = \left(\sum_{i=1}^{N_y} |y_i - \hat{y}_i| \right) / N_y \quad (25)$$

where y_i and \hat{y}_i represent the actual value and predicted traffic flow, respectively; and N^y is the number of all traffic flow data samples.

The flowchart of the IFOA-WNN model is shown in Figure 5. The specific steps are as follows.

- Step 1. Traffic flow data preprocessing. Preprocess the original traffic flow data, the calculate traffic flow data of the section segments by using the mathematical model, divide the preprocessed data into the training set, the validation set and the test set, then normalize them respectively.
- Step 2. Initialize fruit fly swarm parameters. The number of subswarms M is 4, the swarm size N is 10, the number of iterations T_{max} is 100. Set the initial position of the swarm as $[N_{input}, N_{hid}, LR_w, LR_A, LR_B]$, set the initial position of each subswarm as $[N_{input(i)}, N_{hid(i)}, LR_w(i), LR_A(i), LR_B(i)]$, and the fruit fly in the subswarm can be expressed as $[N_{input(i,j)}, N_{hid(i,j)}, LR_w(i,j), LR_A(i,j), LR_B(i,j)]$, $i = 1, 2, \dots, M$, $j = 1, 2, \dots, N$. The search step size L is $[4, 3, 0.002, 0.0002, 0.0002]$, the upper bound of the individual position of the fruit fly swarm ub is $[50, 50, 0.1, 0.01, 0.01]$, and the lower bound of the individual position of the fruit fly swarm lb is $[3, 5, 0, 0, 0]$.
- Step 3. Execute parallel search strategy. The swarm is divided by parallel search strategy, and each subswarm performs the smell search process individually.
- Step 4. Train the WNN model. The training set data and the structural parameters obtained from IFOA are used as the input of WNN, and the WNN is fully trained in the process of forward calculation and error back propagation.
- Step 5. Validate the WNN model. The validation set data is used to get the predicted traffic flow, and the MAE value between the real traffic flow data and the predicted value is calculated.
- Step 6. Calculate the optimal values of the subswarms. The MAE value obtained from the step 5 is used as the smell concentration judgment value $Smell_{(i,j)} = MAE_{P(i,j)}$ of the individual fruit fly. Then, mark the optimal value $bestSmell_i$ in each subswarm.

$$[bestSmell_i, bestIndex_i] = \min(Smell_{i,1}, Smell_{i,2}, \dots, Smell_{i,N}) \quad (26)$$

- Step 7. Select the global optimal value $Smell_{best}$ from the subswarms and update the swarm location coordinates $[N_{input}, N_{hid}, LR_w, LR_A, LR_B]$.

$$Smell_{best} = \min(bestSmell_1, bestSmell_2, \dots, bestSmell_M) \quad (27)$$

$$bestIndex = bestIndex(Smell_{best}) \quad (28)$$

$$N_{input} = bestIndex_{i,N_{input}} \quad (29)$$

$$N_{hid} = bestIndex_{i,N_{hid}} \quad (30)$$

$$LR_w = bestIndex_{i,LR_w} \quad (31)$$

$$LR_A = bestIndex_{i,LR_A} \quad (32)$$

$$LR_B = bestIndex_{i,LR_B} \quad (33)$$

- Step 8. Circulation Stops. When the number of iterations reaches the maximum, the circulation terminates and step 10 is executed; otherwise, go to step 9.
- Step 9. Structural parameters continue to be optimized by IFOA. The position of each sub-swarm $[N_{input(i)}, N_{hid(i)}, LR_{w(i)}, LR_{A(i)}, LR_{B(i)}]$ is updated and the information exchange operation is executed between subswarms according to the group cooperation strategy. Then enter the iteration, repeat step 2 to 8 repeated until the number of iterations reaches.
- Step 10. Finish traffic flow prediction task. Retrain the WNN using the optimal structural parameters $[N_{input}, N_{hid}, LR_w, LR_A, LR_B]$, and then input the test set into the trained WNN model for prediction.

$$N_{input} = bestIndex_{N_{input}} \tag{34}$$

$$N_{hid} = bestIndex_{N_{hid}} \tag{35}$$

$$LR_w = bestIndex_{LR_w} \tag{36}$$

$$LR_A = bestIndex_{LR_A} \tag{37}$$

$$LR_B = bestIndex_{LR_B} \tag{38}$$

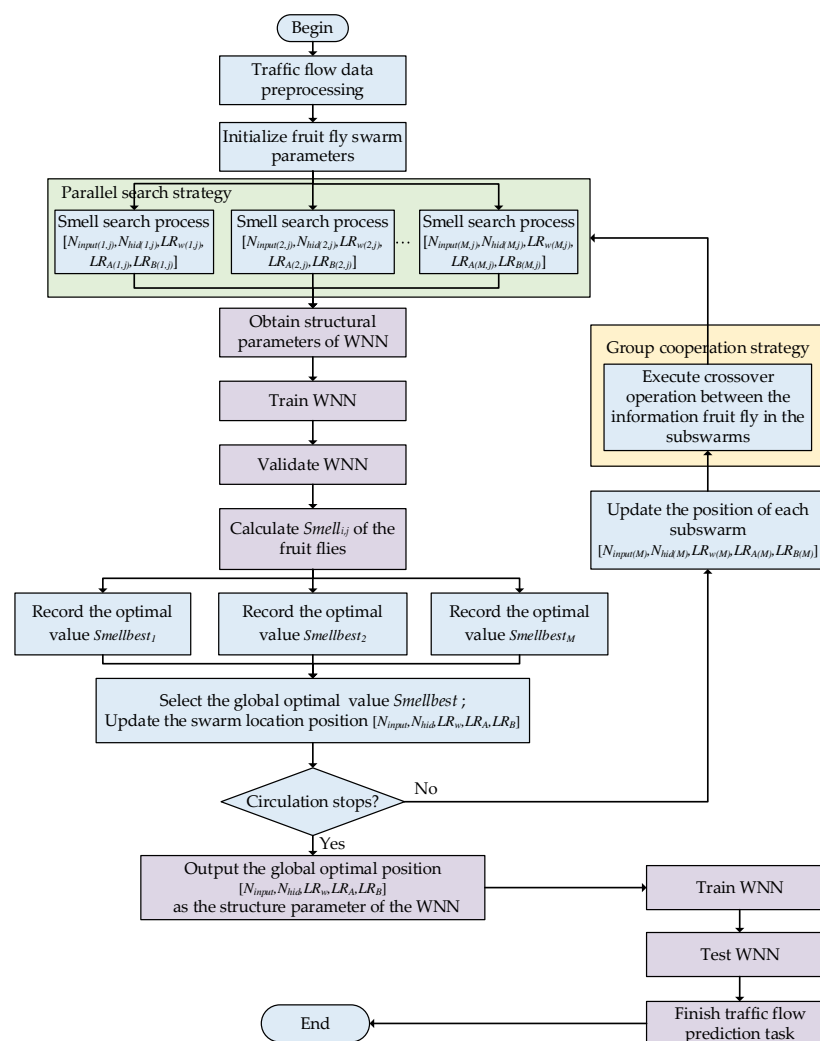
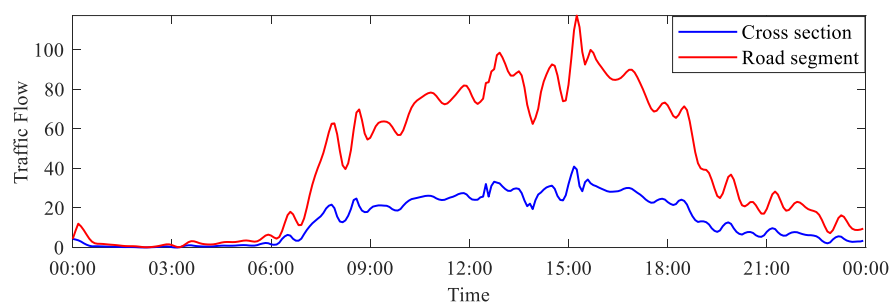


Figure 5. The flowchart of IFOA-WNN prediction model.

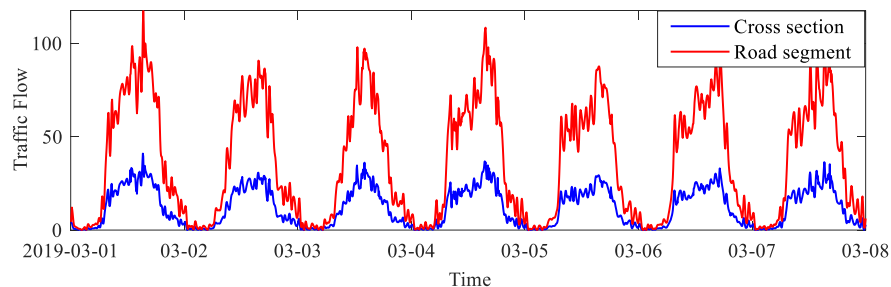
5. Simulation Experiments

5.1. Dataset

The dataset in our experiment is the traffic flow data of California Highway 1 from 1 March 2019 to 31 March 2019, for a total of 31 days. The training set, validation set and test set are divided in the ratio of 6:2:2. The traffic flow data from 1 March to 19 March are selected as the training set, the traffic flow data from 20 March to 25 March as the validation set, and the traffic flow data from 26 March to 31 March as the test set. Since this dataset is a cross section dataset, we use the mathematical model mentioned in Section 2 to calculate the traffic flow data in the road segment scene. The one-day and one-week traffic flow comparison of the road segment and the cross-sectional lane is shown in Figure 6. It can be seen that the traffic flow of the road segment is larger in magnitude, more time-correlated, and time-lagged.



(a)



(b)

Figure 6. The traffic flow comparison of the road segment and the cross section. (a) The traffic flow comparison in a day. (b) The traffic flow comparison in a week.

5.2. Compared Methods

To better demonstrate the prediction performance of the IFOA-WNN model, the BPNN, recurrent neural network (RNN), WNN, and a hybrid model based on WNN with an improved whale optimization algorithm (IWOA-WNN) are selected as baseline methods. The details of the baseline methods are as follows.

- (1) BPNN is a classic neural network model. The input layer, hidden layer units are set to 6 and 15, respectively. The activation function is sigmoid function, and the learning rate is set to 0.01.
- (2) RNN is suitable for time series prediction. The input layer, hidden layer units are set to 6 and 15, respectively. The activation function is tanh function, and the learning rate is set to 0.01.
- (3) WNN is an improved BPNN network. The input layer, hidden layer units are set to 6 and 15, respectively, and the learning rate is set to 0.01. The connection weight

learning rate LR_w , the translation factor learning rate LR_A , and the scaling factor learning rate LR_B are set 0.01.

- (4) IWOA-WNN is a hybrid framework network. The swarm size N is set to 10, the number of iterations T_{\max} is set to 100, the upper bound ub and the lower bound lb of the individual position of the swarm are set to $[50, 50, 0.1, 0.01, 0.01]$ and $[3, 5, 0, 0, 0]$.

We use the traffic flow data from the past 30 min to predict the traffic flow in the next 5 min.

5.3. Evaluation Metric

Mean absolute error (MAE), mean absolute percentage error (MAPE), and root mean square error (RMSE) are selected as evaluation functions to measure the prediction effect of the model, defined as follows.

$$\text{MAPE} = \frac{100\%}{N_y} \sum_{i=1}^{N_y} \left| \frac{y_i - \hat{y}_i}{y_i} \right| \quad (39)$$

$$\text{RMSE} = \sqrt{\left(\sum_{i=1}^{N_y} (y_i - \hat{y}_i)^2 \right) / N_y} \quad (40)$$

where y_t and \hat{y}_t represent the predicted value and actual value, respectively; N_y is the number of all traffic flow data sample. The lower value of MAE, RMSE, and MAPE means that the proposed model has higher accuracy and stronger predictive ability.

5.4. Experiments Analysis

In this study, the IFOA-WNN model for traffic flow prediction in road segments scene is constructed, and the BPNN, RNN, WNN and IWOA-WNN models are introduced as comparison models. The analysis of experiment results is mainly divided into two parts.

- (1) The prediction performance comparison of different NNs models

The wavelet basis function is applied as the activation function of the WNN, and choosing an appropriate wavelet basis function is of great help for the WNN to obtain accurate traffic flow prediction results. The Mexican-hat wavelet function and the Morlet wavelet function have better prediction effects on time series data, so the evaluation metrics of the Mexican-hat wavelet function and the Morlet wavelet function are shown in Table 1. The better values are marked in bold in the Table 1. The MAE, RMSE, and MAPE values of Morlet are better than the Mexican-hat wavelet function. Therefore, the Morlet wavelet function is selected as the activation function of the WNN in our experiments.

Table 1. Evaluation metrics of WNN using two different activation functions.

Activation Function	MAE	RMSE	MAPE (%)
Mexican-hat	3.43	4.31	10.32
Morlet	3.06	3.99	9.12

The evaluation metric of the BPNN, RNN, and WNN models are shown in Table 2. The better values are marked in bold in the Table 2. The traffic flow data of road segments have strong temporal correlation. The MAE, RMSE, and MAPE value of the WNN are smaller than the RNN and BPNN models, indicating that the average error between the predicted value and the true value of WNN is the smallest. Compared with BPNN, WNN has obvious prediction performance, e.g., the MAPE value of the WNN drops by 3.1% compared to the BPNN. The main reason is that the BPNN takes the traffic flow data as a common training sample, while the RNN and WNN models take the traffic flow data as a time series. At the same time, the prediction effect of WNN is also slightly better than RNN, which is due to the better time-frequency characteristics of the wavelet basis function.

Although RNN can capture the time correlation of the traffic flow, the prediction result of RNN exists a certain lag, leading to a decrease in its accuracy.

Table 2. Prediction performance of the BPNN, RNN, and WNN.

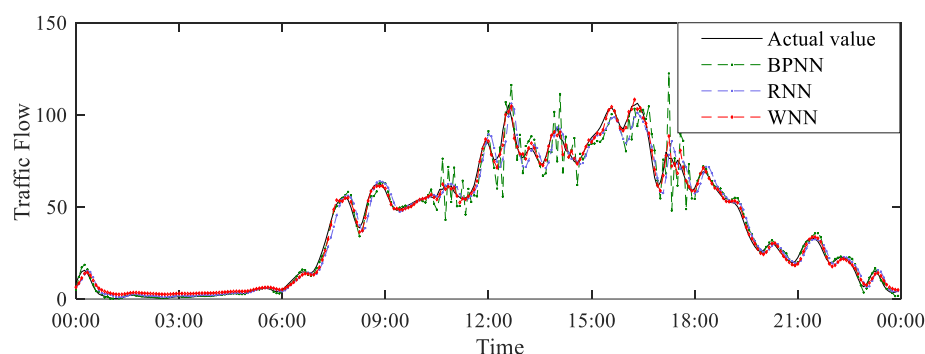
Compared Models	MAE	RMSE	MAPE (%)
BPNN	3.34	4.24	10.22
RNN	4.16	5.43	9.43
WNN	3.06	3.99	9.12

To intuitively display the prediction effect of the three models, 10 sample data are randomly selected from the test set, and the bias between the predicted value and the real traffic flow of the ten sample data is calculated in Table 3. The better biases are marked in bold in the Table 3. From it, we can see that the prediction accuracy of WNN is higher than RNN and BPNN.

Table 3. The predicted value and real traffic flow of the BPNN, RNN, and WNN.

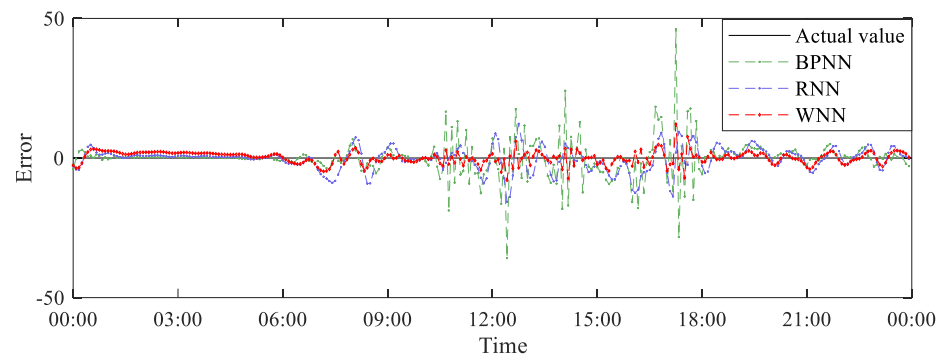
Sample	Actual Data	WNN		RNN		BPNN	
		Predicted Value	Bias (%)	Predicted Value	Bias (%)	Predicted Value	Bias (%)
5	14.01	14.47	3.26%	15.27	9.02%	16.10	14.92%
65	5.61	5.84	4.15%	5.47	3.27%	5.18	7.68%
99	39.84	41.82	4.97%	46.23	16.04%	39.67	0.44%
123	55.07	54.63	0.80%	54.76	0.56%	52.39	4.86%
138	55.85	55.83	0.03%	54.70	2.05%	59.80	7.07%
174	77.12	80.3	4.12%	76.06	1.37%	80.9	4.90%
175	74.56	76.30	2.33%	76.46	2.55%	87.37	17.19%
244	30.26	30.07	0.63%	28.99	4.20%	31.88	5.35%
261	28.64	31.05	8.41%	31.28	9.22%	33.64	17.47%
281	13.77	14.21	3.20%	15.65	13.65%	13.85	0.58%

The prediction results and prediction errors of the WNN, BPNN, and RNN are shown in Figure 7. As Figure 7a shows, the predicted value of the BPNN in the three prediction models deviates greatly from the real value, indicating that its prediction ability is weak. The prediction results of RNN have a certain lag relative to the actual value, while the prediction results of WNN closely follow the changes in the real traffic flow. Figure 7b presents that the error fluctuation of the WNN is smaller than the BPNN and WNN, indicating that the WNN has more robust stability and better prediction performance.



(a)

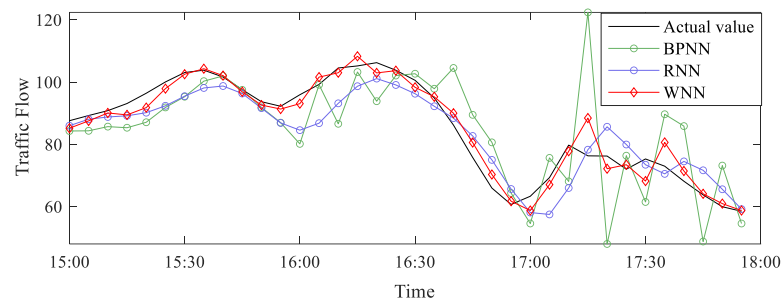
Figure 7. Cont.



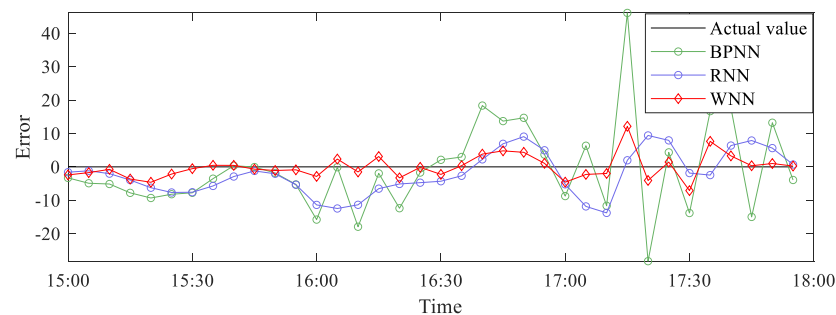
(b)

Figure 7. The prediction performance comparison of the BPNN, RNN, and WNN models in one day. (a) The predicted value and the real traffic flow in one day. (b) The error between the predicted value and the real value in one day.

The changes in traffic flow data are always affected by complex factors. To verify the stability of the prediction models, the BPNN, RNN, and WNN are applied to carry out the prediction task of the evening peak from 15:00 to 18:00. The traffic flow prediction results of the BPNN, RNN, and WNN models are shown in Figure 8. As shown in Figure 8a, the traffic flow of the road segment during the evening peak period is heavy and the change is more obvious compared with the Figure 7a. The prediction result of the WNN is closer to the real traffic flow than the other models, and the prediction error value of the WNN fluctuates less in Figure 8b. This indicates that the WNN has better stability and nonlinear extraction ability, and can make accurate predictions of traffic flow affected by external factors.



(a)



(b)

Figure 8. The prediction performance comparison of the BPNN, RNN and WNN models in one day. (a) The predicted value and the real traffic flow in three hours. (b) The error between the predicted value and the real value in three hours.

(2) The prediction performance comparison of different hybrid NNs models

After the above experiments, the WNN is selected as the traffic flow prediction model. Because the structural parameters of the WNN have a great influence on the prediction performance, the swarm intelligence algorithm is used to optimize the structural parameters of the WNN. In this experiment, two swarm intelligence algorithms, the IWOA and the IFOA, are chosen to optimize the structural parameters of the WNN. Table 4 shows the structural parameters of the WNN optimized by the IWOA and the IFOA.

Table 4. The structural parameters of WNN in two different hybrid frameworks.

Compared Models	N_{input}	N_{hid}	LR_w	LR_A	LR_B
IWOA-WNN	14	23	0.013	0.001	0.001
IFOA-WNN	10	37	0.012	0.004	0.004

The evaluation metric value of WNN, IWOA-WNN and IFOA-WNN are shown in Table 5. The better values are marked in bold in the Table 5. The IWOA-WNN model and the IFOA-WNN model have better prediction results than WNN. The main reason is that the structural parameters that significantly impact the prediction performance are explored in IWOA and IFOA. The MAE, RMSE, and MAPE value of the IFOA-WNN model are all smaller than the IWOA-WNN model, indicating that the IFOA has better optimization ability than the IWOA. The global search strategy and group strategy of IFOA solve the drawback of quickly falling into local optimum, which enhances the quality of the WNN structural parameters and makes the WNN network have stronger nonlinear extraction ability and better prediction effect.

Table 5. Prediction performance of the WNN, IWOA-WNN, and IFOA-WNN.

Compared Models	MAE	RMSE	MAPE (%)
WNN	3.06	3.99	9.12
IWOA-WNN	2.04	2.66	6.12
IFOA-WNN	1.79	2.36	4.62

Ten sample data are randomly selected from the test set, and the bias between the predicted value obtained from the WNN, IWOA-WNN, and IFOA-WNN models and the real traffic flow are recorded. The better biases are marked in bold in the Table 6. As shown in the Table 6, the WNN model improved by the swarm intelligence algorithm has a high prediction performance, which proves that the swarm intelligence algorithm can explore high-quality structural parameters for the WNN. The IFOA-WNN model's accuracy is higher than IWOA-WNN, validating the effectiveness of the IFOA.

Table 6. The predicted value and real traffic flow of the IFOA-WNN, IWOA-WNN, and WNN.

Sample	Actual Data	IFOA-WNN		IWOA-WNN		WNN	
		Predicted Value	Bias (%)	Predicted Value	Bias (%)	Predicted Value	Bias (%)
3	14.83	14.11	4.87%	12.21	17.66%	11.42	22.97%
51	2.61	2.78	6.41%	2.86	9.52%	3.50	34.22%
66	5.79	5.69	1.71%	5.45	5.99%	6.84	18.16%
75	8.01	7.72	3.66%	6.39	20.24%	6.80	15.14%
120	53.47	53.01	0.87%	53.58	0.21%	52.84	1.18%
149	78.97	78.92	0.05%	77.14	2.31%	78.55	0.53%
188	103.86	102.74	1.08%	102.29	1.52%	106.33	2.37%
192	92.27	91.53	0.80%	89.93	2.53%	91.83	0.96%
215	59.99	60.26	0.45%	61.59	2.67%	60.99	1.67%
268	22.78	22.31	2.06%	22.58	0.86%	21.49	5.65%

Figure 9 shows the comparison of the traffic flow prediction results using the WNN model, the IWOA-WNN model, and the IFOA-WNN model. In Figure 9a, the prediction results of the three models all follow the real traffic flow closely, indicating that the three models have great nonlinear extraction ability. Moreover, as shown in Figure 9b, the change of the error of IFOA-WNN is mostly smaller than the WNN model, indicating that the prediction effect of IFOA-WNN is more accurate and stable, which verifies the effectiveness of IFOA in improving the quality of the solution.

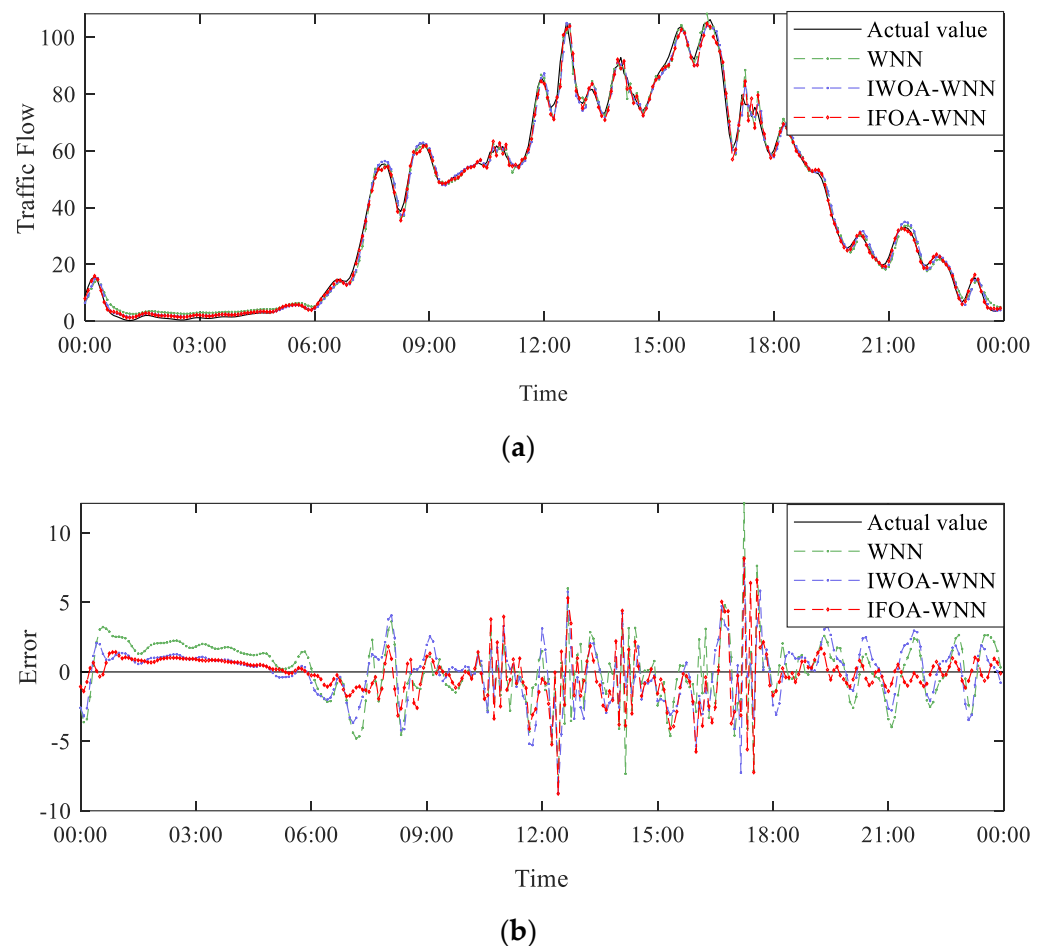


Figure 9. The prediction performance comparison of the WNN, IWOA-WNN, and IFOA-WNN models in one day. (a) The predicted value and the real traffic flow in one day. (b) The error between the predicted value and the real value in one day.

Similarly, to verify the WNN model's predictive stability, three hours of evening peak traffic flow data is used as the input of the IWOA-WNN model and the IFOA-WNN model. The three prediction models can predict the trend of traffic flow change, but the IFOA-WNN model has great following effect and accurate prediction performance in Figure 10a. As shown in Figure 10b, the IFOA-WNN model can better suppress the error of the low-frequency part, indicating that it has better frequency characteristics. On the other hand, it also shows that the IFOA-WNN model can describe the nonlinear characteristic of traffic flow and obtain the frequency domain characteristics to improve accuracy and stability.

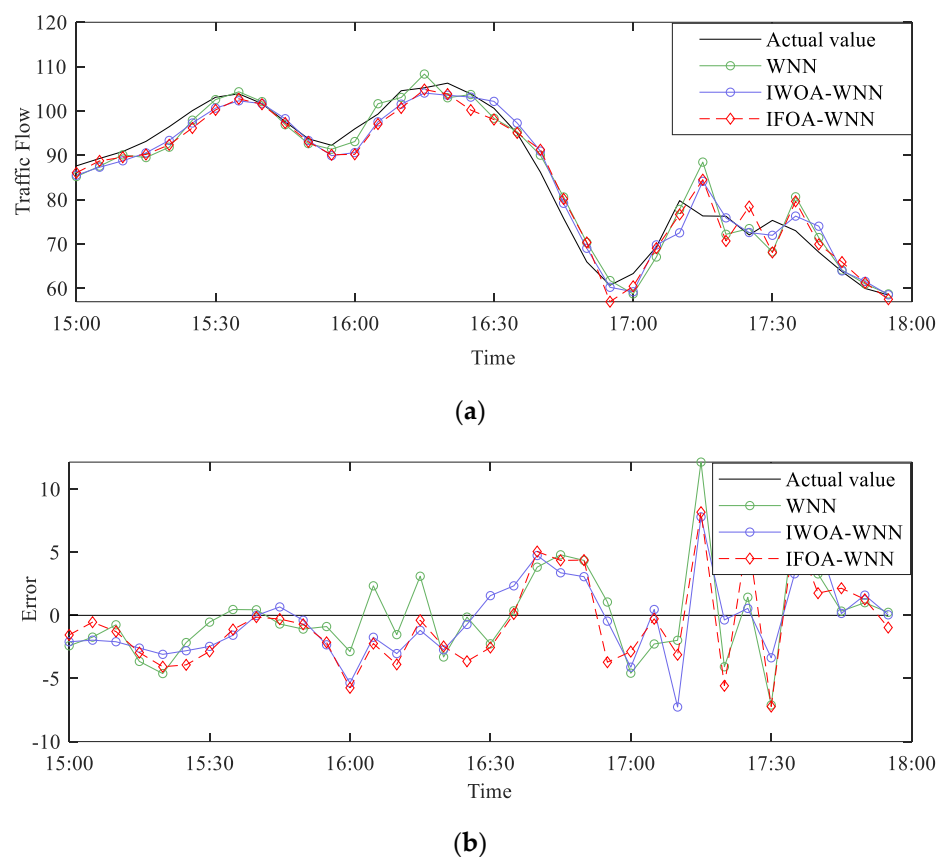


Figure 10. The prediction performance comparison of the WNN, IWOA-WNN and IFOA-WNN models in three hours. (a) The predicted value and the real traffic flow in three hours. (b) The error between the predicted value and the real value in three hours.

6. Conclusions

In this study, the mathematical model of the traffic flow in the road segments is first established, and the traffic flow data of the cross section is used to calculate the traffic flow data of the road segments. Then, the WNN is applied to finish the traffic flow prediction task. Since the WNN is sensitive to the initial weight and wavelet factor, so the IFOA based on parallel search strategy and group cooperation strategy is designed to optimize the structural parameters of WNN. Compared with the BPNN, RNN, WNN and IWOA-WNN models, the experiments' results show that our proposed IFOA is superior to other swarm intelligence algorithms, and in the IFOA-WNN hybrid model, the IFOA can find high-quality structural parameters for the WNN, thereby improving the prediction accuracy of the model and convergence speed.

This paper only considers the temporal characteristic of traffic flow and does not consider the spatial characteristic. In future work, the spatio-temporal feature can be introduced into the input matrix to get more prior knowledge, which has great benefits in improving the prediction performance.

Author Contributions: Conceptualization, Q.Z.; methodology, Q.Z.; software, C.L.; validation, H.Z.; formal analysis, C.Y.; investigation, F.S.; data curation, C.Y.; writing—original draft preparation, C.Y.; writing—review and editing, C.L.; visualization, F.S.; funding acquisition, H.Z. All authors have read and agreed to the published version of the manuscript.

Funding: This research was funded by Natural Science Foundation of Hubei Province of China grant number [2019CFB571].

Institutional Review Board Statement: Not applicable.

Informed Consent Statement: Not applicable.

Data Availability Statement: Not applicable.

Conflicts of Interest: The authors declare no conflict of interest.

References

1. Wu, Q.; Jiang, Z.; Hong, K.; Liu, H.; Yang, L.T.; Ding, J. Tensor-based recurrent neural network and multi-modal prediction with its applications in traffic network management. *IEEE Trans. Netw. Serv. Manag.* **2021**, *18*, 780–792. [[CrossRef](#)]
2. Liao, L.; Hu, Z.; Zheng, Y.; Bi, S.; Zou, F.; Qiu, H.; Zhang, M. An improved dynamic Chebyshev graph convolution network for traffic flow prediction with spatial-temporal attention. *Appl. Intell.* **2022**, *32*, 1–13. [[CrossRef](#)]
3. Okutani, I.; Stephanedes, Y.J. Dynamic prediction of traffic volume through Kalman filtering theory. *Transp. Res. Pract. B-Methodol.* **1984**, *18*, 1–11. [[CrossRef](#)]
4. Smith, B.L.; Williams, B.M.; Oswald, R.K. Comparison of parametric and nonparametric models for traffic flow forecasting. *Transp. Res. Pract. C-Emerg. Technol.* **2002**, *10*, 303–321. [[CrossRef](#)]
5. Jian, W.; Wei, D.; Guo, Y. New Bayesian combination method for short-term traffic flow forecasting. *Transp. Res. Pract. C-Emerg. Technol.* **2014**, *43*, 79–94.
6. Wang, H.; Liu, L.; Dong, S.; Qian, Z.; Wei, H. A novel work zone short-term vehicle-type specific traffic speed prediction model through the hybrid emd–arima framework. *Transp. B-Transp. Dyn.* **2015**, *4*, 159–186. [[CrossRef](#)]
7. Garg, N.; Mangal, S.K.; Saini, P.K.; Dhiman, P.; Maji, S. Comparison of ann and analytical models in traffic noise modeling and predictions. *Acoust. Aust.* **2015**, *43*, 179–189. [[CrossRef](#)]
8. Chen, X.Q.; Wu, S.B.; Shi, C.J.; Huang, Y.; Yang, Y.; Ke, R.; Zhao, J. Sensing data supported traffic flow prediction via denoising schemes and ann: A comparison. *IEEE Sens. J.* **2020**, *23*, 14317–14328. [[CrossRef](#)]
9. Alqatawna, A.; Álvarez, A.M.R.; García-Moreno, S.S.C. Comparison of multivariate regression models and artificial neural networks for prediction highway traffic accidents in spain: A case study. *Transp. Res. Pt. C-Emerg. Technol.* **2021**, *58*, 277–284. [[CrossRef](#)]
10. Sharma, B.; Kumar, S.; Tiwari, P.; Yadav, P.; Nezhurina, M.I. Ann based short-term traffic flow forecasting in undivided two lane highway. *J. Big Data.* **2018**, *5*, 48. [[CrossRef](#)]
11. Ledoux, C. An urban traffic flow model integrating neural networks. *Transp. Res. Pt. C* **1997**, *5*, 287–300. [[CrossRef](#)]
12. Poli, R.; Kennedy, J.; Blackwell, T. Particle swarm optimization. *Swarm Intell.* **2007**, *1*, 33–57. [[CrossRef](#)]
13. Harik, G.R.; Lobo, F.G.; Goldberg, D.E. The compact genetic algorithm. *IEEE Trans. Evol. Comput.* **1999**, *3*, 287–297. [[CrossRef](#)]
14. Dorigo, M.; Caro, G.D. Ant colony optimization: A new meta-heuristic. *Evol. Comput.* **1999**, *2*, 1470–1477.
15. Karaboga, D.; Gorkemli, B.; Ozturk, C.; Karaboga, N. A comprehensive survey: Artificial bee colony algorithm and applications. *Artif. Intell. Rev.* **2014**, *42*, 21–57. [[CrossRef](#)]
16. Tsao, P.W. A new Fruit fly optimization algorithm: Taking the financial distress model as an example. *Knowl.-Based Syst.* **2012**, *26*, 69–74.
17. Mirjalili, S.; Lewis, A. Grey wolf optimizer. *Adv. Eng. Softw.* **2014**, *69*, 46–61. [[CrossRef](#)]
18. Mirjalili, S.; Lewis, A. The whale optimization algorithm. *Adv. Eng. Softw.* **2016**, *95*, 51–67. [[CrossRef](#)]
19. Zhang, Q.Y.; Qian, H.; Chen, Y.P. A short-term traffic forecasting model based on echo state network optimized by improved fruit fly optimization algorithm. *Neurocomputing* **2020**, *416*, 117–124. [[CrossRef](#)]
20. Liu, X.J.; Qin, X.L. A probability-based core dandelion guided dandelion algorithm and application to traffic flow prediction. *Eng. Appl. Artif. Intell.* **2020**, *96*, 103922. [[CrossRef](#)]
21. Chan, K.Y.; Dillon, T.S.; Chang, E. An intelligent particle swarm optimization for short-term traffic flow forecasting using on-road sensor systems. *IEEE Trans. Ind. Electron.* **2013**, *60*, 4714–4725. [[CrossRef](#)]
22. Abolghasem, S.N.; Parima, M.; Maryam, S. Short-term traffic flow prediction using the modified elman recurrent neural network optimized through a genetic algorithm. *IEEE Access.* **2020**, *8*, 217526–217540.
23. Yan, H.; Zhang, T.; Qi, Y.; Yu, D.J. Short-term traffic flow prediction based on a hybrid optimization algorithm. *Appl. Math. Model.* **2022**, *102*, 385–404. [[CrossRef](#)]
24. Li, H.T. Network traffic prediction of the optimized bp neural network based on glowworm swarm algorithm. *Int. J. Syst. Sci.* **2019**, *7*, 64–70. [[CrossRef](#)]
25. Peng, Y.N.; Wan, L.X. Short-term traffic volume prediction using GA-BP based on wavelet denoising and phase space reconstruction. *Physica. A* **2020**, *549*, 123913. [[CrossRef](#)]
26. Mahshid, F.; Shadan, G.; Kayvan, T.; Alex, D.C.; Alireza, S. A wavelet feature-based neural network approach to estimate electrical arc characteristics. *Electr. Power Syst. Res.* **2022**, *208*, 107893.
27. Yang, H. Wavelet neural network with soa based on dynamic adaptive search step size for network traffic prediction. *Int. J. Opt.* **2020**, *224*, 165322. [[CrossRef](#)]
28. Chen, Q.; Song, Y.; Zhao, J. Short-term traffic flow prediction based on improved wavelet neural network. *Neural Comput. Appl.* **2021**, *33*, 8181–8190. [[CrossRef](#)]
29. Jiang, W.H.; Wu, X.G.; Gong, Y.; Yu, W.X.; Zhong, X.H. Holt–Winters smoothing enhanced by fruit fly optimization algorithm to forecast monthly electricity consumption. *Energy* **2020**, *193*, 116779. [[CrossRef](#)]

30. Qiao, L.; Liu, Y.; Zhu, J. Application of generalized regression neural network optimized by fruit fly optimization algorithm for fracture toughness in a pearlitic steel. *Eng. Fract. Mech.* **2020**, *235*, 107105. [[CrossRef](#)]
31. Ruby, B.; Priti, M.; Piyush, S.; Prashant, S.; Manish, S. Implementation of fruit fly optimization algorithm to escalate the attacking efficiency of node capture attack in wireless sensor networks. *Comput. Phys. Commun.* **2020**, *149*, 134–145.
32. Ma, C.; Dai, G.; Zhou, J. Short-term traffic flow prediction for urban road sections based on time series analysis and LSTM_BiLSTM method. *IEEE Trans. Intell. Transp. Syst.* **2021**, *23*, 5615–5624. [[CrossRef](#)]